Proceedings of the 11th World Congress on Mechanical, Chemical, and Material Engineering (MCM'25)

Barcelona, Spain -Paris, France - August, 2025

Paper No. HTFF 232 DOI: 10.11159/htff25.232

Thermal Dispersion Impact on Hybrid Nanofluid Saturated Mixed Convection over Horizontal Cone

Nayema Islam Nima

Independent University, Bangladesh (IUB) Plot 16 Aftab Uddin Ahmed Rd, Dhaka-1229, Bangladesh Email: nayema@iub.edu.bd

Abstract- This study investigates the effects of thermal dispersion on mixed convection flow of a hybrid nanofluid over a horizontal cone, where the base fluid is ethylene glycol and the suspended nanoparticles are cylindrical-shaped alumina (Al₂O₃) and silica (SiO₂). The hybrid nanofluid, composed of equal volume fractions of alumina and silica, demonstrates markedly enhanced thermal performance compared to the mono nanofluid containing alumina alone. The governing nonlinear partial differential equations are transformed into a system of ordinary differential equations using similarity transformations and are solved numerically via the Bvp4c method. The results reveal that suction significantly enhances the heat transfer rate by thinning the thermal boundary layer, whereas injection has a diminishing effect, particularly in the forced convection regime. Thermal dispersion tends to reduce heat transfer by weakening the temperature gradient near the surface, with stronger effects observed in forced and mixed convection regions. Moreover, an increase in the Biot number consistently enhances heat transfer, especially as the flow shifts toward free convection dominance. These findings highlight the potential of hybrid nanofluids for advanced thermal management applications, including cooling technologies, heat exchangers, and energy systems where efficient convective heat transfer is essential.

Keywords: hybrid nanofluid, ethylene glycol, forced convection, thermal dispersion, suction/injection

1. Introduction

Nanofluids—suspensions of nanosized particles in conventional base fluids have gained widespread attention in thermal engineering due to their superior thermal conductivity, viscosity modulation, and ability to enhance convective heat transfer performance. Building upon this, hybrid nanofluids, formed by mixing two or more types of nanoparticles, have demonstrated enhanced energy transport capabilities due to synergistic effects between the constituent nanoparticles [1], [2]. Recent research has confirmed the thermal superiority of hybrid nanofluids across a range of geometries and physical effects. Shaik et al. [1] demonstrated that Cu–Graphene/water hybrid nanofluids offer improved stability and thermophysical behavior, making them suitable for high-performance cooling applications. Sarfraz et al. [2] compared thermal performance using different conductivity models and found that hybrid nanofluids consistently outperform mono nanofluids in enhancing heat transfer rates. Further, Shahid et al. [3] highlighted the role of mixed convection in hybrid nanofluid-filled cavities and emphasized the impact of thermal boundary configurations. Asghar et al. [4] extended this understanding by incorporating magnetic field effects and heat generation/absorption terms, showing how external forces and thermal sources further influence hybrid nanofluid transport mechanisms.

However, one critical aspect that remains underexplored is the effect of thermal dispersion, which encompasses enhanced thermal spreading due to both microscopic conduction and fluid particle mixing. This phenomenon becomes especially relevant in complex geometries like cones, domes, and cylindrical surfaces, where curvature introduces unique boundary layer characteristics. For instance, Wahid et al. [5] examined radiative mixed convection flow of hybrid nanofluids near a vertical flat plate and highlighted the sensitivity of heat transfer to Soret and Dufour effects—mass and thermal diffusion mechanisms akin to dispersion. Similarly, Riaz et al. [6] investigated modified hybrid nanofluid flow in a vertical cylinder, underscoring how geometric curvature and mixed convection jointly modulate temperature and velocity fields. Rashid et al. [7] presented a detailed analysis of hybrid nanofluid flow over a stretching surface, illustrating the significant role of suction and magnetic fields in regulating heat transfer under mixed convection. These findings

collectively underscore the importance of boundary conditions, external fields, and geometry-specific behavior in nanofluid systems.

This study uniquely contributes to this evolving field by exploring the combined effects of thermal dispersion, suction/injection, and Biot number on hybrid nanofluid flow over a horizontal cone a geometry that remains less studied despite its relevance in solar collectors, heat exchanger fins, and energy harvesting devices. The nanofluid consists of cylindrical alumina (Al₂O₃) and silica (SiO₂) nanoparticles suspended in ethylene glycol, and the system is modeled using similarity transformations with numerical solutions via the Bvp4c method. The comparison between mono and hybrid nanofluids under different convection regimes provides insight into optimizing heat transfer in advanced thermal systems.

2. Mathematical modelling

Consider a steady, laminar, mixed convection boundary layer flow over a semi-vertically angled horizontal cone embedded in a porous medium saturated with fluid, where the ambient temperature is denoted by T_{∞} . The surface of the cone is subjected to convective heating from a warm hybrid nanofluid maintained at a constant temperature T_f , with a spatially varying heat transfer coefficient $h_f(x^*)$. Employing the Boussinesq approximation, the governing conservation equations namely, the continuity, momentum and energy equations as Ferdows et al. [8], Sarfraz et al. [9] are formulated, incorporating thermal dispersion effects and a convective boundary condition at the surface.

$$\frac{\partial (ru^*)}{\partial x^*} + \frac{\partial (rv^*)}{\partial y^*} = 0 \tag{1}$$

$$\frac{\partial u^*}{\partial y^*} = -\frac{\partial}{\partial x^*} \left(\frac{gk(\rho \beta_{hbnf})}{\mu_{hbnf}} (T - T_{\infty}) \cos \varpi \right)
u^* \frac{\partial T}{\partial x^*} + v^* \frac{\partial T}{\partial y^*} = \frac{\partial}{\partial y^*} \left(\alpha^*_{e} \frac{\partial T}{\partial y^*} \right)$$
(2)

Boundary conditions

 $v^* = v_w^*, -k_{hbnf} \frac{\partial T}{\partial y} = h_f(x^*)(T_f - T) \text{ at } y = 0$ $u^* \to u_\infty^*, T \to T_\infty \text{ at } y \to \infty$ (4)

(3)

Where
$$\alpha_e^* = \alpha_{hbnf} + a^* du = \frac{k_{hbnf}}{(\rho_{cp})_{hbnf}} + a^* du$$
 (5)

Here α_e^* , α_{hbnf} , a^* are effective thermal, constant thermal and coefficient of thermal dispersion respectively.

 a^* value is between $\frac{1}{7}$ to $\frac{1}{3}$.

Transformations

$$\eta = \left(\frac{u_{\infty}^{*}}{\alpha_{f} x^{*}}\right)^{0.5} y, \psi = \left(\alpha_{f} u_{\infty}^{*}\right)^{0.5} r^{*} f(\eta), \theta(\eta) = \frac{T - T_{\infty}}{T_{f} - T_{\infty}}$$
(6)

Using (5) and (6), transformed equations (1-4) are as follows:

$$f'' = \frac{\frac{(\rho \beta_{hbnf})}{(\rho \beta_{f})} \lambda_{m}^{3} \frac{\eta}{2} \theta'}{\frac{\mu_{hbnf}}{\mu_{f}}} \lambda_{m}^{3} \frac{\eta}{2} \theta'$$

$$\frac{\frac{k_{hbnf}}{k_{f}}}{(\rho_{cp})_{hbnf}} \theta'' + \frac{1}{2} f \theta' + a^{*} P e_{d}^{*} (f' \theta'' + f'' \theta') = 0$$

$$(8)$$

Boundary Conditions

$$f = s^*, \frac{k_{hbnf}}{k_f} \theta' = -B_{iot} (1 - \theta(0)) \quad \text{at } \eta = 0$$
$$f' = 1, \theta \to 0 \quad \text{at } \eta \to \infty$$

Defining parameters

(9)

$$\lambda_{m} = \frac{Ra_{x}^{\frac{1}{3}}}{Pe_{x}^{\frac{1}{2}}}, Ra_{x} = \frac{gk(\rho \beta_{f}(T_{f} - T_{\infty})x^{*}\cos\varpi}{\mu_{f}\alpha_{f}}, Pe_{x} = \frac{u_{\infty}^{*}x^{*}}{\alpha_{f}}, B_{iot} = \frac{-h_{f}\alpha_{f}^{0.5}}{k_{f}u_{\infty}^{0.5}}, h_{f}(x^{*}) = x^{-0.5}h_{f}(x^{*})$$

Table 1. Nanofluid properties
$$\rho_{nf} = ((1-\phi_{1})\rho_{f} + \phi_{1}\rho_{Al_{2}o_{3}}) \\ (\rho_{c_{p}})_{nf} = ((1-\phi_{1})(\rho_{c_{p}})_{f} + \phi_{1}(\rho_{c_{p}})_{Al_{2}o_{3}}) \\ (\rho_{\beta})_{nf} = ((1-\phi_{1})(\rho_{\beta})_{f} + \phi_{1}(\rho_{\beta})_{Al_{2}o_{3}}) \\ (\rho_{\beta})_{nf} = ((1-\phi_{1})(\rho_{\beta})_{f} + \phi_{1}(\rho_{\beta})_{Al_{2}o_{3}}) \\ \frac{k_{nf}}{k_{f}} = \frac{k_{Al_{2}o_{3}} + (r_{1}-1)k_{f} - (r_{2}-1)(k_{f}-k_{Al_{2}o_{3}})}{k_{Al_{2}o_{3}} + (r_{1}-1)k_{f} + (k_{f}-k_{Al_{2}o_{3}})} \\ \mu_{nf} = \frac{\mu_{f}}{(1-\phi_{1})^{2.5}}, \nu_{nf} = \frac{\mu_{nf}}{\rho_{nf}}$$

$$\frac{k_{bf}}{k_{f}} = \frac{k_{Al_{2}o_{3}} + (r_{1}-1)k_{f} - (r_{1}-1)(k_{f}-k_{Al_{2}o_{3}})\phi_{1}}{k_{Al_{2}o_{3}} + (r_{1}-1)k_{f} - (r_{1}-1)(k_{f}-k_{Al_{2}o_{3}})\phi_{1}} \\ \mu_{hbnf} = \frac{\mu_{f}}{(1-\phi_{1})^{2.5}}, \nu_{hbnf} = \frac{\mu_{hbnf}}{\rho_{hbnf}}$$

According to Sarfraz et al. [9], the shape factor for the nanoparticles $r_1 = 6$ is selected in the aforementioned expressions, as our study focuses on cylindrical-shaped nanoparticles.

Table 2. Physical properties of nanoparticles and basefluid

Physical	Nar	Base Fluid	
Properties			
	Alumina	Silica	Ethylene glycole
c_p	765	745	2430
k	46	1.38	0.253
β	0.85×10^{-6}	0.55×10^{-6}	0.57×10^{-6}
ρ	3970	2220	1115

$$P_{1} = \frac{\mu_{hbnf}}{\mu_{f}}, P_{2} = \frac{(\rho_{\beta})_{hbnf}}{(\rho_{\beta})_{f}}, P_{3} = \frac{(\rho_{c_{p}})_{hbnf}}{(\rho_{c_{n}})_{f}}, P_{4} = \frac{k_{hbnf}}{k_{f}}$$

3. Numerical solution

The transformed system of nonlinear ordinary differential equations, obtained via similarity transformations from the governing partial differential equations, is solved numerically using MATLAB's built-in boundary value problem solver bvp4c. This method is well-suited for solving two-point boundary value problems with high accuracy.

To implement the solution, the system of higher-order ODEs is first reduced to a system of first-order differential equations. The equations, boundary conditions, and an initial mesh are then defined in MATLAB using function handles. An initial guess for the solution is provided based on physical intuition or simplified cases. The bvp4c solver applies a collocation method with adaptive mesh refinement to solve the system iteratively. Convergence is ensured by monitoring residual errors and adjusting the mesh until the solution meets the desired tolerance.

Now substituting η for x^* and also considering

$$h_1 = f, h_2 = f', h_3 = \theta, h_4 = \theta'$$

The first order equations are

$$\begin{split} \frac{dh_1}{dx} &= f' = h_2, \\ \frac{dh_2}{dx} &= f'' = \frac{p_2}{p_1} * \lambda^3 * \frac{\eta}{2} * h_4 \\ \frac{dh_3}{dx} &= \theta' = h_4, \\ \frac{dh_4}{dx} &= \theta'' = (-0.5 * h_1 * h_4 - a * Pe_d * (\frac{p_2}{p_1} * \lambda^3 * \frac{\eta}{2} * h_4)) / (\frac{p_4}{p_3} + a^* * Pe_d * h_2) \end{split}$$

Boundary conditions

$$hp(1) - s^* = 0$$
, $hq(2) - 1 = 0$
 $p_4 * hp(4) + B_{iot} * (1 - hp(3)) = 0$, $hq(3) = 0$

HTFF 232-4

The variable hp denotes the boundary condition on the left side, whereas hq corresponds to the right-side boundary. To validate the accuracy of the present numerical results, a comparative analysis was performed against the findings of Ferdows et al. [8] for a specific case, as shown in Table 3. The excellent agreement between the two sets of results confirms the reliability and precision of the current computational approach.

	101		3 (), (,	11 12	
B_{iot}	Pe_d	f'(0)		$-\theta'(0)$		
		Present study	Ferdows et al.	Present study	Ferdows et al.	
			[8]		[8]	
10000000	0	1.0000	1.0000	0.5644	0.5644	
1.5	0	1.0000	1.0000	0.4101	0.4100	
1.5	10	1 0000	1 0000	0.2539	0.2538	

Table 3. Biot number B_{iot} and Dispersion effect on f'(0), $-\theta'(0)$ for the regular fluid $(\phi_1 = \phi_2 = 0)$

4. Results discussion

In this analysis, the nanofluid consists of 4% volume fraction of alumina nanoparticles ($\phi_1 = 0.04$, $\phi_2 = 0.00$), while the hybrid nanofluid comprises 2% alumina and 2% silica nanoparticles ($\phi_1 = 0.02$, $\phi_2 = 0.02$). **Figure 1(a)** illustrates the effects of suction and injection on the velocity profile. Suction reduces the boundary layer thickness by drawin fluid toward the surface, while injection thickens it by introducing fluid. The hybrid nanofluid exhibits a thinner boundary layer and steeper velocity gradient than the mono nanofluid, due to enhanced thermal and momentum diffusivity from the combined nanoparticles. **Figure 1(b)** shows that increasing thermal dispersion enhances velocity near the surface by promoting energy distribution within the fluid. Overall, hybrid nanofluids demonstrate superior flow and heat transfer characteristics under mixed convection and dispersion effects compared to mono nanofluids.

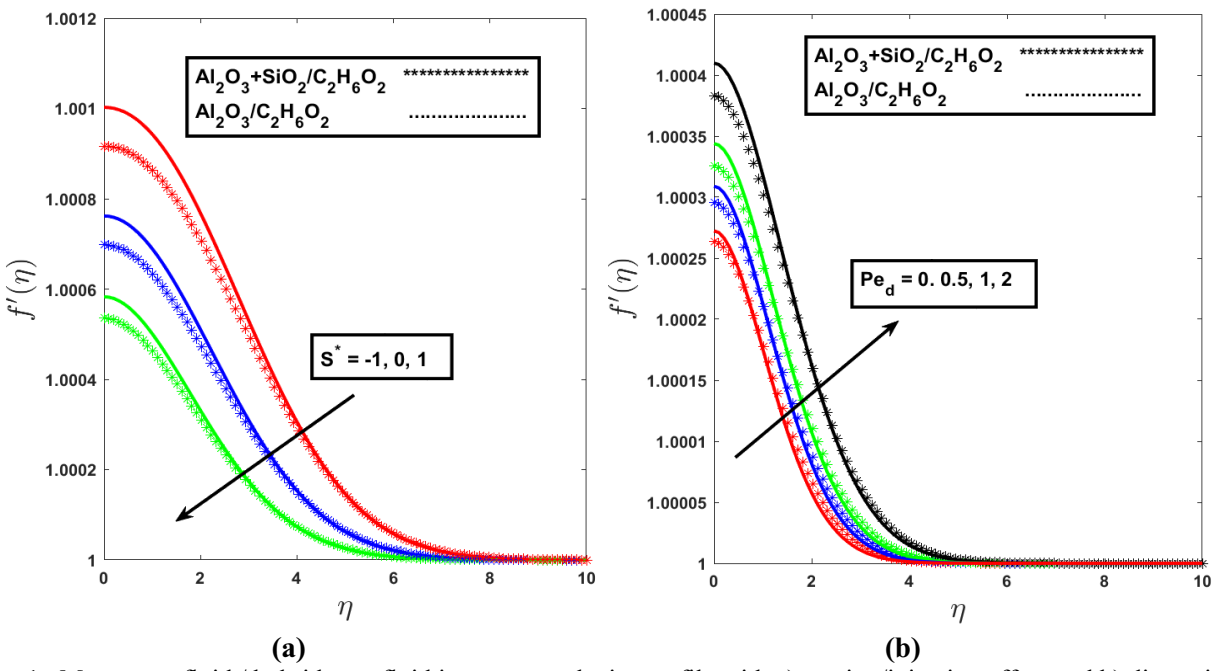
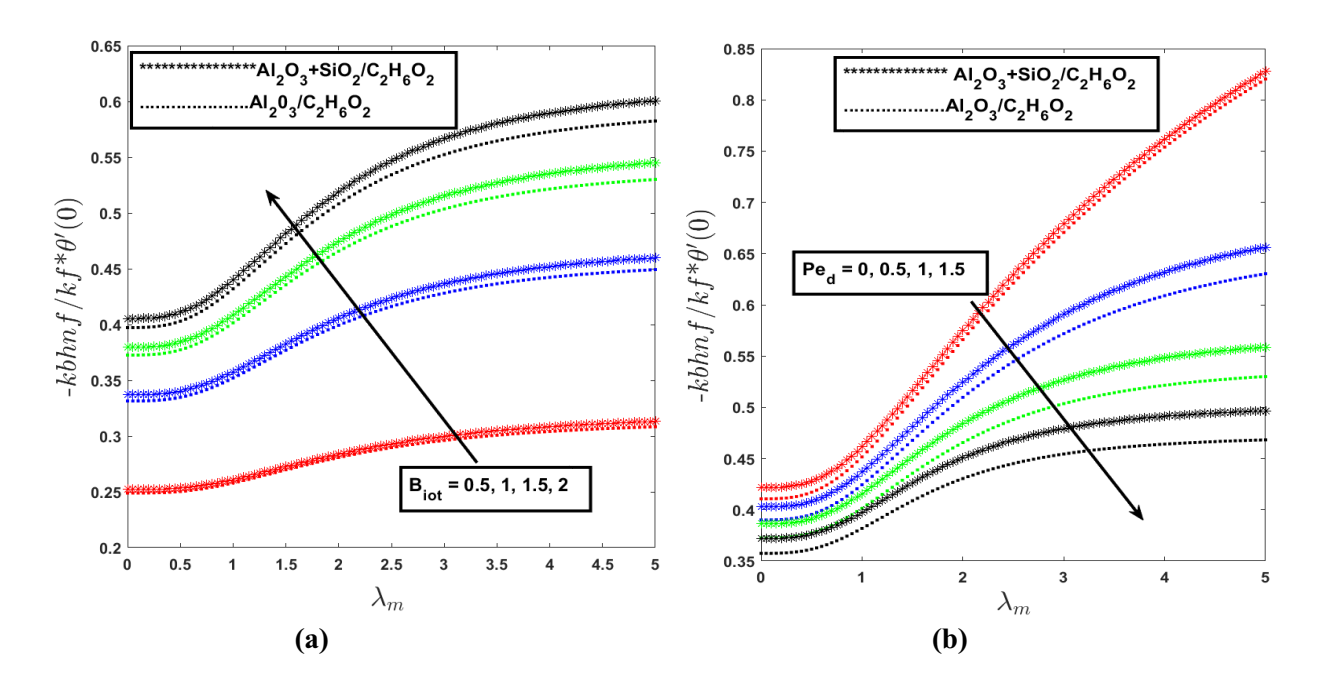


Fig. 1. Mono nanofluid / hybrid nanofluid impact on velocity profile with a) suction/injection effect and b) dispersion effect.

Figure 2(a) shows the influence of the Biot number on heat transfer for different values of the mixed convection parameter, where $\lambda_m = 0$ represents pure forced convection and higher values indicate increasing buoyancy effects. As the Biot number increases from 0.5 to 1.5, the heat transfer rate rises due to stronger convective exchange at the surface. The hybrid nanofluid consistently achieves higher heat transfer than the mono nanofluid, emphasizing the enhanced thermal performance resulting from the combined nanoparticles, especially under stronger mixed and free convection conditions.

Figure 2(b) illustrates the effect of thermal dispersion on the heat transfer rate. The results indicate that lower dispersion leads to higher heat transfer, while greater dispersion weakens the surface temperature gradient and thus reduces heat transfer. When λ_m lies within the range 0 to 1, corresponding to the transition zone from forced to mixed convection, the heat transfer rate is comparatively lower. However, as λ_m increases beyond 1, entering the free convection-dominant regime, a noticeable rise in the heat transfer rate is observed, particularly for the hybrid nanofluid. This trend underscores the hybrid nanofluid's enhanced responsiveness to buoyancy-driven flow mechanisms, which become more significant in free convection conditions. Figure 2(c) illustrates the effect of the suction/injection parameter sss on the heat transfer rate. Suction ($s^* = -1$) enhances heat transfer by thinning the thermal boundary layer, while injection ($s^* = 1$) reduces it by introducing fluid at the surface. The case of no mass transfer ($s^* = 0$) shows a slight decrease. These effects are most prominent in the forced convection region ($\lambda_m \approx 0$), diminish under mixed convection, and become negligible in the free convection regime. The influence of suction is notably more beneficial for the hybrid nanofluid, reflecting its superior thermal transport properties.



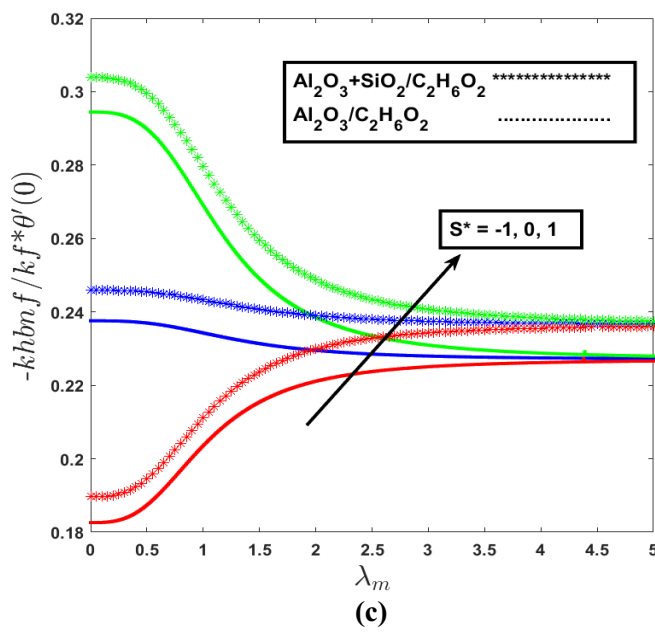


Fig. 2. Effect of mono nanofluid and hybrid nanofluid on heat transfer rate with the variation of a) biot number b) dispersion parameter c) suction/injection parameter

4. Conclusion

The present investigation provides a comparative analysis of mono and hybrid nanofluids under the influence of mixed convection, thermal dispersion, and suction/injection. The key outcomes are as follows:

- Hybrid nanofluids demonstrate superior heat transfer performance compared to mono nanofluids due to enhanced thermal and momentum diffusivity from combined nanoparticles.
- Suction significantly enhances heat transfer by reducing boundary layer thickness, while injection decreases it; these effects are most prominent in the forced convection regime.
- Increasing thermal dispersion tends to reduce the heat transfer rate by diminishing the surface temperature gradient, with a more pronounced effect under forced and mixed convection.
- A higher Biot number leads to increased heat transfer, particularly as the system transitions from forced to free convection.
- The impact of hybrid nanofluids becomes more evident in the mixed and free convection regimes, indicating their greater sensitivity to buoyancy-driven flow conditions.

References

- [1] A.H. Shaik, S. Chakraborty, S. Saboor, K.R. Kumar, A. Majumdar, M. Rizwan, M. Arıcı, and M.R. Chandan, "Cu-Graphene water-based hybrid nanofluids: synthesis, stability, thermophysical characterization, and figure of merit analysis," *J. Therm. Anal. Calorim.*, vol. 149, pp. 2953–2968, 2024.
- [2] M. Sarfraz, M. Yasir, and M. Khan, "Exploring dual solutions and thermal conductivity in hybrid nanofluids: a comparative study of Xue and Hamilton–Crosser models," *Nanoscale Adv.*, vol. 5, pp. 6695–6704, 2023.
- [3] M. A. Shahid, M. Dayer, , I. Hashim, A. I. Alsabery & S. Momani, "Numerical investigation of multiphase flow effects on mixed convection in partially heated hybrid nanofluid-filled cavity," *J. Therm. Anal. Calorim.*, 2024. https://doi.org/10.1007/s10973-023-12860-4

- [4] A. Asghar, A. F. Chandio, Z. Shah, N. Vrinceanu, W. Deebani, M. Shutaywi, & L. A. Lund, "Magnetized mixed convection hybrid nanofluid with effect of heat generation/absorption and velocity slip condition," *Heliyon*, vol. 9, no. 2, e13189,2023.
- [5] N. S. Wahid, N. M. Arifin, N. S. Khashi'ie, I. Pop, N. Bachok, & M. E. H. Hafidzuddin, "Hybrid nanofluid radiative mixed convection stagnation point flow past a vertical flat plate with Dufour and Soret effects," *Mathematics*, vol. 10, no. 16, p. 2966, 2022.
- [6] A. Riaz, A. Abbasi, K. Al-Khaled, S.U. Khan, W. Farooq, E.S.M.T. El-Din, "A numerical analysis of the transport of modified hybrid nanofluids containing various nanoparticles with mixed convection applications in a vertical cylinder," *Front. Phys.*, vol. 10, 1018148, 2022.
- [7] A. Rashid, M. Ayaz, and S. Islam, "Numerical investigation of the magnetohydrodynamic hybrid nanofluid flow over a stretching surface with mixed convection: A case of strong suction," *Adv. Mech. Eng.*, vol. 15, no. 6, 2023. https://doi.org/10.1177/16878132231179616.
- [8] M. Ferdows, B. Alshuraiaan, and N. I. Nima, "Effects of non-Darcy mixed convection over a horizontal cone with different convective boundary conditions incorporating gyrotactic microorganisms on dispersion," *Sci. Rep.*, vol. 12, no. 1, p. 16581, 2022.
- [9] M. Sarfraz, M. Yasir, and M. Khan, "Multiple solutions for non-linear radiative mixed convective hybrid nanofluid flow over an exponentially shrinking surface," *Sci. Rep.*, vol. 13, no. 1, p. 3443, 2023.